

# Science with Bolometer Arrays on the GBT

*v.01may03 Brian S. Mason*

*v.24jun03 rev.2*

## Abstract

We examine the science which can be done with bolometer arrays on the GBT, considering both the Penn Array (a 3mm, 64 pixel bolometer array current under construction at the University of Pennsylvania) and a notional 6400 pixel array. We identify a number of areas where such an instrument could make important contributions. A key unique role for the GBT is that of a continuum search engine for ultra-luminous, dusty galaxies at high redshifts.

## Contents

<b>1</b>	<b>Introduction</b>	<b>1</b>
<b>2</b>	<b>Generalities</b>	<b>2</b>
2.1	Bolometer Arrays on the GBT . . . . .	2
2.2	Mapping Speeds . . . . .	3
2.3	Angular Resolution & Confusion . . . . .	4
2.4	Arrays & Anomalous Refraction . . . . .	7
<b>3</b>	<b>Stellar &amp; Planetary Systems</b>	<b>8</b>
3.1	Star Formation . . . . .	8
3.2	Pre-Main-Sequence Stars . . . . .	10
3.3	Debris Disks & Extra-Solar Planets . . . . .	11
3.4	Our Solar System . . . . .	12
<b>4</b>	<b>Galaxy Clusters &amp; the Sunyaev-Zel'dovich Effect</b>	<b>13</b>
<b>5</b>	<b>The Origin &amp; Evolution of Galaxies</b>	<b>16</b>
<b>6</b>	<b>Summary &amp; Conclusions</b>	<b>19</b>
<b>A</b>	<b>Appendix: Other Instruments</b>	<b>22</b>

## 1 Introduction

The principal feature which distinguishes the Green Bank Telescope (GBT) from other large single-dish telescopes is its capacity for operations at frequencies up to  $\sim 115$  GHz. When the phase III operations are achieved, the GBT will have the largest effective collecting area of any telescope at a wavelength of 3mm ( $\sim 2000$  m<sup>2</sup>). When ALMA is fully operational it will exceed this by a factor of about three. However single dish telescopes have the advantage that the collecting area can be cheaply and effectively leveraged in comparison to

interferometers by large-format focal plane arrays. Emerging technologies permit focal planes with  $\sim 10,000$  or more pixels at millimeter and sub-millimeter wavelengths, *e.g.*, SCUBA-2 which will have  $\sim 30,000$  pixels in total divided between  $450\,\mu\text{m}$  and  $850\,\mu\text{m}$ . A fully-sampled GBT focal plane can easily contain up to  $\sim 6,000$  pixels at 3mm (Norrod & Srikanth, 1999), offering the prospect that the GBT mapping speed at 3mm could eventually exceed that of ALMA by more than three orders of magnitude.

The Penn Array Receiver (PAR) is a 64-pixel bolometer array for the 80 to 100 GHz window; it is funded and well into its detailed design phase, with a target deployment date on the GBT of winter 2004/2005. The technologies and issues for a large format array are likely to be very similar to those for the Penn Array, so this instrument is a pathfinder for future, larger format arrays. In this memo we consider the PAR as an illustration of what can be achieved on the GBT at 3mm within the next 3 years; we also consider the prospects for a notional 6,000 pixel array on the GBT.

The purpose of this memo is to review the scientific justification for these instruments and assess their likely scientific impact. We begin with a general consideration of the bolometer arrays on the GBT. Next we look in detail at several areas where a large array on the GBT is expected to have a significant impact: star formation & planetary systems (including our Solar System); Cosmology & the Sunyaev-Zel'dovich Effect (SZE); and high- $z$  galaxies. Finally we summarize our conclusions and highlight areas where the GBT can potentially play a prominent role. Throughout we pay attention to other relevant instrumental capabilities with an eye to identifying the GBT's unique contribution.

## 2 Generalities

### 2.1 Bolometer Arrays on the GBT

The Penn Array will consist of 64 elements arranged in an  $8 \times 8$  square. Each beam will have a FWHM of  $\sim 8''$  on the sky; it is meant to be an approximately fully sampled ( $0.5f_\lambda$ ) array, so the spacing between adjacent beams will be  $\sim 4''$ . The instantaneous field of view is then  $32'' \times 32''$ . The most recent loading and efficiency estimates from Mark Devlin and Simon Dicker yield per detector sensitivities  $343\,\mu\text{Jy}\,\text{t}_{\text{sec}}^{-\frac{1}{2}}$ . Some scalability is being built into the Penn Array, *i.e.*, there is excess capacity in the multiplexer and extra space in the focal plane. It is likely that a factor of a few increase in the number of pixels will be obtainable at a fairly modest cost.

For purposes of this study we also consider a hypothetical Large Array consists of a scaled-up version of the Penn Array: an  $80 \times 80$ , fully sampled array of TES bolometers with comparable per-pixel sensitivities. This yields an instantaneous FOV of  $5'.3 \times 5'.3$ . Using the results tabulated by Norrod & Srikanth (1999) we can determine the optical properties of such an array. At the edges of the field the peak sidelobe level is up 10 dB from  $-30$  dB to  $-20$  dB in relation to the maximum gain. The optical efficiency of an element at a radius of

2'.65 differs negligibly from that of an element at the on-axis focus position—the primary effect of the offset is to redistribute power amongst the sidelobes anisotropically. We neglect the effects of the reimaging optics (lyot stop, lenses, etc), which needs further investigation. This fiducial case conveniently corresponds to a 100-fold increase in mapping speed, and a 10-fold increase in the depth to which you can map a fixed area in a fixed time, over the Penn Array.

It is also a conservative “future case”. The  $N = 6,000$  number of Norrod & Srikanth is for the case of a  $3f_\lambda$  array of feedhorns. The TES arrays can be much more closely packed in the focal plane—the Penn Array elements have  $0.5f_\lambda$  spacing. If other considerations such as price, wiring, or reimaging optics are not limitations, then 36,000 pixel ( $12' \times 12'$  FOV) camera should then be feasible. Such an instrument would have about  $10^4$  times the mapping speed of ALMA at 3mm. This comparison assumes zero-overhead (on-the-fly) mapping with both instruments. Except in § 2.4 we do not consider this case further.

## 2.2 Mapping Speeds

We outline the calculation of the RMS noise level in a Penn Array map of a  $1^\circ \times 1^\circ$  field with 6 hours of integration. The beam volume for an  $8''$  FWHM beam is  $2\pi\sigma^2 = 72 \text{ arcsec}^2$ , so a  $1 \text{ deg}^2$  area contains  $1.8 \times 10^5$  independent beams. If our  $1^\circ \times 1^\circ$  area were mapped by a single detector, the detector would spend  $6 \times 3600 / (1.8 \times 10^5) = 0.12$  seconds per beam for a noise level of  $343 / \sqrt{0.12} = 987 \mu\text{Jy}$  per beam on the sky. The noise in each detector is uncorrelated, so the final map noise is  $987 \mu\text{Jy} / \sqrt{64} = 123 \mu\text{Jy}$  per beam.

Sensitivities for three other cases of Penn Array observing— all 6 hour integration times, and areas compatible with GBT slew rate limitations— are shown in Table 1. Where appropriate we also tabulate the corresponding sensitivities for a Large Array. The Penn Array cannot map more than  $\sim 64 \text{ deg}^2$  in 6 hours as it is limited by the maximum slew-rate of the GBT ( $40'/\text{sec}$ ). The Large Array would be able to map an area 10 times larger than this ( $640 \text{ deg}^2$ ). This case is also shown in the table. These calculations neglect the effects of residual systematic errors and the likely necessity of estimating instrumental parameters.

Generally note that for an equal number of feeds, a large telescope has an advantage of  $D^2$  in time in mapping a fixed area to a fixed rms flux density per beam over a smaller telescope— this is an advantage in large-area *point source* finding projects. This comes from  $D^4$  (in time) increase in sensitivity to unresolved sources, versus the necessity of observing  $D^2$  more pointings with the large telescope. There is an advantage of  $N_{\text{feed}}$  in time also. For an equal number of feeds the surface brightness sensitivity of large and small single dishes are equal. For mapping extended objects the larger dish will impose more stringent constraints on instrument stability and data processing because the (small) pixels we need to be coherently processed for sensitive measurements of extended structures; however current total power imaging techniques are fairly sophisticated (*e.g.* Fixsen et al., 2000; Stompor et al., 2002). Large-area searches for unresolved or marginally resolved sources are clearly then a major strength

Field Size	PAR Sens. [ $\mu$ Jy]	Large Array Sens. [ $\mu$ Jy]
$30'' \times 30''$	1	—
$5' \times 5'$	10	1
$1^\circ \times 1^\circ$	120	12
$8^\circ \times 8^\circ$	980	100
$25^\circ \times 25^\circ$	—	310

Table 1: Cases of Penn Array sensitivities and data volumes. All assume: 6 hours of integration. For slew-speed limited OTF mapping the Penn Array can cover a maximum area of  $64 \text{ deg}^2$  in 6 hours if we allow 50% re-sampling of the sky to improve atmosphere & systematics rejection. Assuming both focal planes are square, the notional Large Array can cover 10 times this, albeit to a deeper level. We have assumed a per-detector sensitivity of  $343 \mu\text{Jy sec}^{1/2}$ . **Erratum: Jim Condon has pointed out that the rms for point source detection in table 1 and elsewhere in this memo should be  $\sqrt{2}$  higher than it is — I used beam volume instead of variance beam volume (24jun03).**

of the GBT; it will also be strongly competitive for imaging extended objects whose spectral energy distributions (SEDs) peak in the mm regime (such as cold dust and CMB). The extended-source and point source mapping speeds for both cases increase as  $N_{feed}$ .

For a number of reasons it is almost certain that large bolometer arrays on the GBT and other instruments will primarily operate in a raster-scan/On-the-fly mode. One advantage of this approach is that it minimizes observing (scan start/stop *etc.*) overheads. Most interferometers do not currently support such mapping modes, nor is the software in place to analyze such data although it is specified by the ALMA SSR group. Also, depending on the configuration, very rapid sampling of the correlator would be needed if the long baselines are to be used, possibly limiting slew speeds. Generally it is more straightforward to use large arrays on single dishes for big continuum maps.

Figures 1 and 2 compare the sensitivity of the GBT/Penn Array combination to a selection of other instruments for extragalactic and galactic targets respectively. In these plots a set of representative SEDs are normalized to the RMS achieved by the Penn Array in a one hour map of one square degree. These figures demonstrate that for extragalactic and many Galactic sources the Penn Array will be competitive with the next generation of planned instrumentation. Sources for sensitivity estimates are tabulated in Appendix A.

### 2.3 Angular Resolution & Confusion

Bolometer receivers on large-aperture telescopes will quickly integrate down to very faint flux densities and we are led to consider confusion. Suppose that sources down to a threshold  $S_o$  in flux density are identified and subtracted

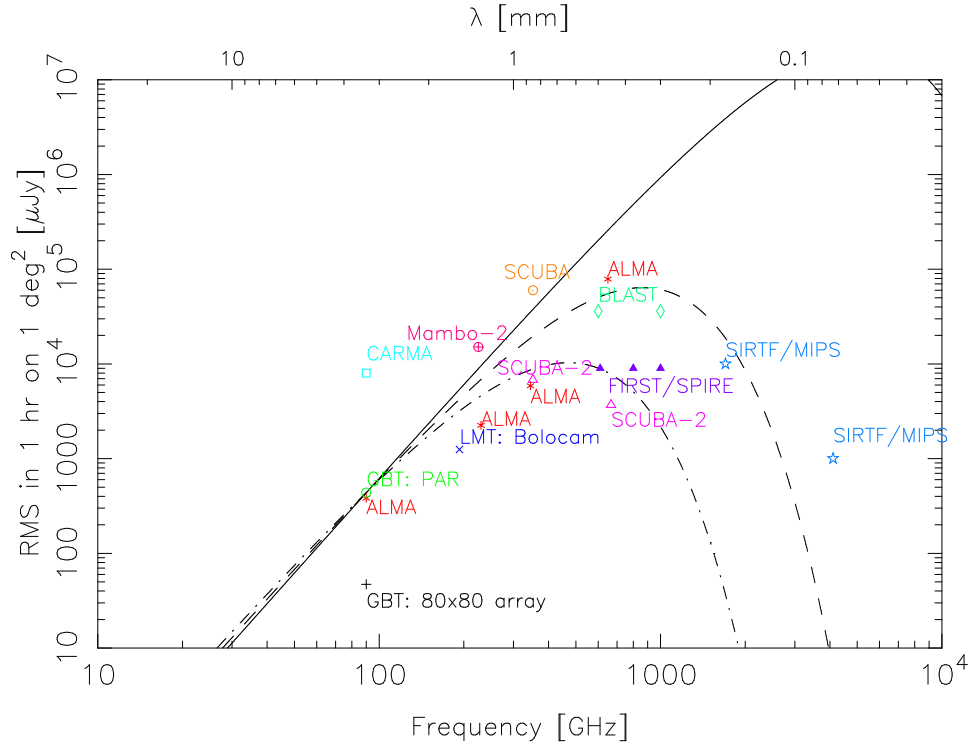


Figure 1: A comparison of the mapping speeds of major mm and submm instruments. Modified blackbody curves are chosen to be characteristic of star-forming galaxies, assuming  $\beta = 1.35$ ,  $T = 58$  K (Yun & Carilli, 2002). Redshifts are  $z = 0$  (solid),  $z = 5$  (dashed), and  $z = 10$  (dot-dashed). All curves are normalized to the  $1\sigma$  RMS achieved by the Penn Array on the GBT on one square degree. In this time on this area, SIRTIF and Herschel are expected to be confusion limited. An  $80 \times 80$  3mm array on the GBT is also expected to be nearly confusion limited in this time.

from a map. Further suppose that the map is populated with sources which follow  $N(> S) = N_o(S/S_o)^{-\lambda}$ . The rms confusion  $\sigma_{conf}$  due to sources below that threshold is then for a Gaussian beam (eg Rohlfs et al., 2000)

$$\sigma_{conf} = S_o \sqrt{\frac{\Omega_B}{2} N_o \frac{\lambda}{2 - \lambda}} \quad (1)$$

where  $\frac{\Omega_B}{2}$  is the variance beam volume, or roughly half the Gaussian beam volume. This assumes that  $\lambda < 2$ . Blain et al. (2002) estimate the 3mm source counts to be

$$N(> S) \sim 200 \text{ deg}^{-2} \left( \frac{S}{200 \mu\text{Jy}} \right)^{-1.6} \quad (2)$$

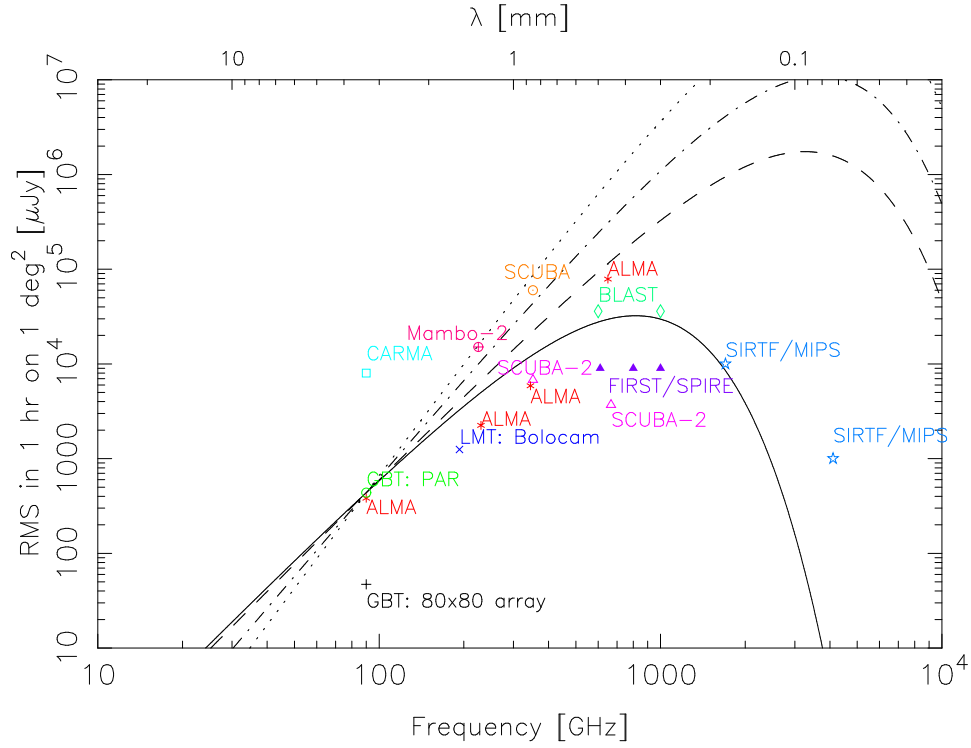


Figure 2: Similar to figure 1, except the modified blackbody curves are chosen to be characteristic of Galactic targets. These are: cold pre-protostellar core ( $\beta = 1$ ,  $T = 10$  K—solid line);  $T\tau$  star ( $\beta = 1$ ,  $T = 40$  K—dashed line); evolved YSO ( $\beta = 1.5$ ,  $T = 40$  K—dash-dot line); and molecular cloud dust emission ( $\beta = 2$ ,  $T = 40$  K).

This then predicts that a map will be confusion-limited at the  $5\sigma$  level for  $S_o = 30 \mu\text{Jy}$ , *i.e.*, if you remove all peaks brighter than  $30 \mu\text{Jy}$  the residual source confusion is  $\sigma_{conf} = 5 \mu\text{Jy}$ . With a sensitivity of  $343 \mu\text{Jysec}^{1/2}$ , a  $5 \mu\text{Jy}$  RMS is reached in 1.3 hours on one point on the sky ( $30'' \times 30''$  for the Penn Array). The above is may be a conservative estimate since the counts are expected to become shallower at faint flux levels; if  $\lambda = 1$  the  $5\sigma$  map is confusion limited at  $S_o = 3 \mu\text{Jy}$ . The confusion will be a factor of 2–3 higher in massive galaxy clusters due to lensing of background sources (Smail et al., 1997).

In general, the smaller beam of the GBT will give it a lower confusion threshold in comparison to other single-dish mm and sub-mm telescopes. It can be shown that the limiting flux densities ( $S_1, S_2$ ) for two telescopes with different beam sizes ( $\Omega_1, \Omega_2$ ) have the ratio

$$\frac{S_1}{S_2} = \left( \frac{\Omega_1}{\Omega_2} \right)^{1/\lambda} \quad (3)$$

Considering the range  $1 < \lambda < 1.6$ , the GBT can probe 1.5 to 1.9 times as deep as SCUBA (15'' beam at 850  $\mu\text{m}$ ) and 1.2 to 1.4 times as deep as the IRAM 30m (11'' at 1.2 mm). That is, for an arbitrary but fixed SED characterizing the sources, confusion limited maps with the GBT reach 1.2 – 2 times as fainter in flux at any frequency as confusion-limited maps at 850  $\mu\text{m}$  with SCUBA or 1mm with the IRAM 30m. Note that for purposes of imaging extended structures large telescopes have an advantage over small telescopes since you get to clean down to the deeper level before averaging pixels for sensitive estimates of extended emission.

The above estimate is derived from submm galaxy counts. Holdaway et al. (1994) derive

$$N(> S) = 4.2 \times 10^{-3} \text{ deg}^{-2} \left( \frac{S}{1 \text{ Jy}} \right)^{-1.38} \quad (4)$$

from 90 GHz sources brighter than 100 mJy. These are mostly AGN, and they are likely to be a small contribution at these faint levels.

On larger scales SZE distortions from high- $z$  clusters may be a significant unresolved background. Recent arcminute-scale CMB experiments suggest an RMS Compton parameter  $\sigma_y \sim 4 \times 10^{-6}$ , which corresponds to  $\sim 7 \mu\text{Jy}$  per 8'' beam. This signal would have a characteristic scale of  $\sim 1'$ .

## 2.4 Arrays & Anomalous Refraction

A potentially significant uncertainty associated with mm operations at the Green Bank site is the limitations imposed by anomalous refraction. Fully-sampled arrays would seem to open the possibility of using “guide stars” in realtime to correct for pointing errors and anomalous refraction effects, which we now consider. This would require either an agile tertiary or a very large field of view. We consider the maximal case of a  $12' \times 12'$  FOV, for which the instantaneous coverage is  $0.04 \text{ deg}^2$ . The timescale for anomalous refraction events on a 100 meter telescope is  $\sim 10$  seconds or longer (Altenhoff et al., 1987; Olmi, 2001), so assume a cycle time of two seconds, and a one second integration on the reference source per cycle. Require a  $6\sigma$  detection— enough for arcsecond centroiding, but more importantly enough to confidently identify the real source in one out of 36000 pixels. We expect  $N(S_{3mm} > 2 \text{ mJy}) \sim 2 \text{ deg}^{-2}$  (Blain et al., 2002), so one in twelve  $12' \times 12'$  fields would have such a source within it. A smaller array with access to an agile tertiary would also do. The tertiary would require a  $20'$  throw in two axes, however, for one source to be accessible on average for a random sky pointing. This will be difficult to achieve mechanically (see Srikanth, 1991).

On the other hand some projects are naturally well-suited to this technique. Maps of low-mass star forming cores will be arcmin<sup>2</sup> in extent and will have many compact sources brighter than a few mJy, suitable for pointing self-cal. Similarly, deep galaxy surveys could be chosen to be near a sufficiently bright source. This should add a substantial degree of robustness to observations likely to be challenging.

It may also be possible to use total power gradients across the array to estimate anomalous refractive effects. This need not be based on complicated, uncertain, and variable atmospheric models, but could be empirically calibrated on the fly from periodic pointing calibrator observations. Since the relation between the power gradient and the pointing offset should only change on meteorological timescales, the cycle times would not be expected to be very short (10's of minutes, say). Whether this is detectable and usable in the face of other variable gradients while the telescope is scanning (*e.g.*, the ground) remains to be seen.

### 3 Stellar & Planetary Systems

Star formation occurs in visually opaque regions of clouds of gas and dust. Stars form when dense cloud condensations reach a point where gravitational forces overcome the thermal pressure, turbulent motions, and magnetic fields that support the cloud. During the protostellar collapse most protostars appear to form a disk, which helps the young star to grow. At the same time these accretion disks drive powerful outflows, which get rid of excess magnetic energy and angular momentum. The details of what triggers the collapse— and conversely, how molecular clouds are supported against collapse— as well as whether single or multiple star systems are formed, are still rather speculative. Even though the mass of a star largely determines how a star will evolve during its life cycle, we do not know what parameters determines the star's birth mass. Neither do we know what fraction of the initial accretion disks survive to form planetary systems. We know that at least some of these disks survive, because one can still see debris disks surrounding main-sequence stars which may be birth grounds for planets. We also know, from Doppler studies of nearby stars, that many stars are surrounded by planets.

In the next few sections we examine how bolometer arrays on the GBT can contribute to the study of the evolution of stellar and planetary systems.

#### 3.1 Star Formation

Dark and molecular clouds in our Galaxy are sites of ongoing star formation, and are the prime laboratories in which we can study the early stages of the stellar life cycle. These clouds are typically parsecs to a few tens of parsecs in extent which translates into an angular extent of many arcminutes up to degrees (in the case of Orion). Wide-area surveys of these regions with bolometer arrays, typically at short mm or submm wavelengths, have proven very efficient in finding protostars and deeply embedded young stars (*e.g.* Motte et al., 1998; Johnstone & Bally, 1999). Although protostars can be detected in the far infrared, the spatial resolution is poor and the dust emission can be optically thick. The GBT— due to its collecting area, resolution, and the mapping speeds offered by large-format focal plane arrays— can be expected to make vital contributions to this field. We illustrate with two specific cases.



First consider a survey of a nearby star-forming core. Such a survey has been done by Testi & Sargent (1998) at 3mm with the OVRO array. These authors mosaiced a  $5'.5 \times 5'.5$  region in Serpens to an RMS of 0.9 mJy/beam with a beam FWHM of  $5''$ . This required well over 50 hours of integration time. In one half-hour the Penn Array on the GBT should achieve an RMS of  $50 \mu\text{Jy}$  on a  $5' \times 5'$  field.

In addition the extended molecular cloud emission will be imaged. This has characteristic surface brightnesses of 10 MJy/Sr at 1.3 mm, corresponding to  $400 \mu\text{Jy}$  per GBT beam at 3mm for  $\beta = 2$ . Because the dust emission falls off more steeply at long wavelengths for dust in the surrounding cloud cores than for dust in protostellar disks ( $\beta \sim 1$ ) the clump-cloud contrast will be higher than in shorter wavelength maps, providing a complementary view of conditions in the cloud. Filled-aperture telescopes will also provide a much more complete view of the cloud than the highly filtered view provided by interferometers. If the large-scale emission is confusing for some particular study (*e.g.*, protostellar mass function estimation) the maps can be high-pass filtered. This results in some loss of sensitivity, but there is plenty of sensitivity. Similar studies have been done at 1.3 mm with the IRAM 30-m & the MPIfR 19-channel bolometer array (Motte et al., 1998). These authors mapped  $\sim 480 \text{ arcmin}^2$  of  $\rho$  Oph to an RMS of 5 – 10 mJy, requiring some tens of hours. The equivalent RMS at 3mm is 0.4 – 0.8 mJy assuming  $\beta = 1$ . The Penn Array will be able to image this region to 0.1 mJy RMS in  $\sim 2$  hrs, hundreds of times faster than IRAM.

As a second example, consider a blind, large-area Galactic plane survey. At the GBT maximum slew speed of  $40'/\text{sec}$  the Penn Array can map  $10 \text{ deg}^2$  per hour to an RMS of  $\sim 1 \text{ mJy}$ . In 50 hours one could image a reasonable fraction of the Galactic plane. There will be two main classes of objects sought in such a survey:

1. **Isolated low-mass protostars:** These will have surface brightnesses of a few to 20 mJy per beam at 3mm; angular extents are 10s of arcseconds up to 2 arcminutes or so. To reliably detect the fainter ones, smoothing the maps or integrating more deeply would be necessary.
2. **High-Mass Star Forming Regions:** These will have surface brightnesses of a few 10s to a few 100 mJy per GBT 3mm beam, and typical angular extents of a few arcminutes.

Currently high-mass star forming regions are mostly found through secondary tracers (*e.g.*, Ultra-Compact HII), so a large-area mm survey has significant discovery potential. Pre-protostellar cores are expected to be cold (5 – 10 K) and their SEDs will peak at longer wavelengths; mm-wave cameras are the ideal way to search for these objects.

There are a number of other clear applications of bolometer arrays on the GBT:

- Sub-mm observations have been very important in allowing detailed study of the structure of star-forming regions, as well as mass determinations for

the disks surrounding protostars. However some protostars or extremely young stars like IRAS 4 in NGC 1333 still show optically thick dust emission in the sub-mm regime and in this case observations at longer wavelengths are needed to determine the disk masses. Generally it is desirable to sample the continuum flux of protostellar disks at a wide range of frequencies to answer this and other questions, and the high point source sensitivity of the GBT at 3mm will be excellent for this.

- One of the leading star formation models, Shu's inside-out collapse model, suggests that star formation proceeds as an inside out collapse of a cloud core. This should lead to a characteristic radial density distribution proportional to  $r^{-0.5}$  close to the accretion core, and steepen further out, while an isothermal core should have a  $r^{-2}$  dependence. Recent analysis of 850  $\mu\text{m}$  maps (Shirley et al., 2002) suggest that this may not be the case; high-sensitivity, high-resolution observations at 3mm would help clarify the situation.

### 3.2 Pre-Main-Sequence Stars

Many young pre-main-sequence stars (T Tauri, FU Ori and Herbig Ae/Be stars) have been detected in thermal dust emission at 1.3 mm or in the sub-mm regime (Weintraub et al., 1989a; Beckwith et al., 1990; Mannings, 1994). Since young Pre-Main-Sequence (PMS) stars are still embedded in the dust clouds in which they formed, it is essential to map the dust emission, because in order to find the true properties of the circumstellar dust emission one needs to be able to separate the disk emission from that of the surrounding cloud. This can only be done by mapping a region around the star. By mapping the surroundings of young stars one can also ensure that they do not have nearby, even younger companions that can be so deeply embedded that they are not seen in the optical or the near-IR (Aspin et al., 1994; Sandell & Weintraub, 1994; Henning et al., 1998). High resolution mapping with SCUBA shows that many PMS stars have extended dust envelopes or disks (Weintraub et al., 1999). This is to be expected, as high resolution molecular line maps show that these stars are surrounded with extended disks, that show Keplerian motions (Weintraub et al., 1989b; Mannings et al., 1997). Furthermore, high resolution imaging with the HST and large ground based telescopes show circumstellar disks seen in silhouette against bright reflection nebulae with radii of 300 - 700 AU. Yet high resolution aperture synthesis studies at 3 mm find the dust emission to be unresolved, or at most only partially resolved (Simon & Guilloteau, 1992; Koerner et al., 1993) suggesting that current aperture synthesis telescopes lack sensitivity to probe the cold outer regions of these proto-planetary disks. These extended envelopes show 850  $\mu\text{m}$  surface brightnesses of 50 - 150 mJy per 15'' beam, and have steep ( $\beta \sim 2$ ) spectra. They would then be expected to show 3mm surface brightnesses of  $\sim 80 - 240 \mu\text{Jy}$  per GBT beam. The Penn Array could make a  $2' \times 2'$  map of the region around a T Tauri star to a sensitivity of 10  $\mu\text{Jy}$  in just one hour. An  $80 \times 80$  array could do this in less than a minute.

Some T Tauri stars themselves have 3mm flux densities of 20 to 100 mJy and so accurate photometry is possible in a few seconds with a bolometer system on the GBT. Many T Tauri stars, however, do not have bright mm emission (see, *e.g.*, Hogerheijde et al., 2002). The Penn Array on the GBT will be the most sensitive ground-based instrument to study these systems in the near future, and will be able to detect much less massive disks than possible with current instrumentation.

These studies show that the dust emission has a surprisingly flat spectral energy distribution, suggesting that the thermal dust emission has a lower dust emissivity index than what one sees in diffuse interstellar dust. The dust emission in some T Tauri stars suggests that the flat spectral energy distribution could be due to very large dust grains, perhaps the start of a planetary system. In a few extreme cases it is clear that the dust is still partly optically thick in the sub-mm and it is therefore important to extend the observations to longer wavelengths. The GBT can map the total extent of the dust emission far more efficiently than any existing mm-aperture synthesis telescope. By combining results from the GBT with observations from other single dish telescopes like the IRAM 30 m at 1.3mm and the JCMT at 850 and 450 $\mu$ m it will be possible to derive much more detailed information about the dust distribution and mass of these protoplanetary disks. By studying stars of different ages one can find out whether there exists a clear transition period when the dust grains assemble into planetesimals and when the disk is cleared by planets.

The SIRTf Multi-band Imaging Photometer (MIPS) will image with a  $4' \times 4'$  FOV out to 160 $\mu$ m, encompassing the peak of the dusty disk SEDs around 70 $\mu$ m. It will more quickly detect the sorts of dusty disks that you expect. However the Penn Array on the GBT at 3mm will in the near term be the next fastest instrument, and valuable for determining the properties of the disk SEDs in the long-wavelength regime. At FIR wavelengths SIRTf's spatial resolution is also three to seven times worse than that of the GBT at 3mm. It can be expected that ground-based 3mm observations will be useful for follow-up on SIRTf observations of T-Tauri stars.

### 3.3 Debris Disks & Extra-Solar Planets

The Infrared Astronomical Satellite (IRAS) mission found that more than 15% of nearby, main-sequence stars have a far-infrared excess over and above the emission expected from the stellar photosphere. Three of these, Vega ( $\alpha$  Lyr), PsA and  $\beta$  Pictoris were resolved by IRAS at 60 $\mu$ m with diameters of  $\sim 30$  arcsec (300 - 500 AU). Optical and mid-infrared imaging of  $\beta$  Pic, showed that the star is surrounded by a massive optically thick disk (Paresce & Burrows, 1987). These stars are thought to be signposts of extrasolar planetary systems, and their morphologies, related to a timeline, give important insights into the process of planet formation. Debris disks are difficult to observe in the optical/infrared— the dust is cold and it is difficult to separate the dust emission from starlight.

Observations in the mm/sub-mm regime are much more sensitive to debris

disks than optical observations. Prototypical Vega-like stars, Vega, Fomalhaut,  $\beta$  Pictoris, and  $\epsilon$  Eri, are very striking in the sub-millimeter (see, *e.g.*, Holland et al., 1998). Fomalhaut shows a nearly edge-on disk around the central star as one would expect to see from a star with a planetary debris disk. The  $850\,\mu\text{m}$  maps show thermal dust emission with a major axis of  $41''$  (315 AU), a minor axis of  $18''$ , and an integrated flux density  $S_{850} = 81 \pm 7\,\text{mJy}$ ; these observations required 5h with the JCMT. Quite unexpectedly,  $\beta$  Pictoris and Vega show bright blobs far from the central star; another prototypical Vega-like star,  $\epsilon$  Eri, shows a nearly pole-on ring-like disk structure with a bright region in the ring Greaves et al. (1998). These regions may be indicative of already formed planets or ongoing planet forming regions. More imaging observations of Vega-like stars is important to know whether this is a generic feature of planetary debris systems.

The debris disks consist of large dust particles, perhaps even planets. They are characterized by SEDs which approach thermal black bodies ( $1 < \beta < 0$ ), possibly indicative of cm-sized grains. At 3mm the emission is therefore much stronger than what it would be from normal interstellar dust. The GBT will have both better sensitivity and spatial resolution than any other telescope currently in operation for mapping planetary debris disks, and could therefore make an important contribution to our understanding of how planets form. Consider the case of Fomalhaut again, which has a measured opacity spectral index  $\beta \sim 0.8$  (Holland et al., 2003). We then expect an integrated  $S_{3\text{mm}} \sim 31\,\text{mJy}$ , or an average surface brightness of 3mJy per GBT beam. The Penn Array can make a  $1' \times 1'$  map with sub-mJy RMS in less than one minute. This map will have nearly twice the resolution of a SCUBA  $850\,\mu\text{m}$  map. In this case since the targets are small a much larger-format array would not be very helpful.

There are now several tens of known extrasolar planets detected by Doppler surveys of nearby FGKM dwarfs. Some interest was generated by an early claim of a dust disk around one such star, 55 Cancri. Later SCUBA observations did not support this, resolving instead two probable background sources. 3mm GBT observations would be useful for such observations; the sensitivity would be comparable or slightly better (Fig 2) but the resolution higher.

### 3.4 Our Solar System

The discovery Trans-Neptunian Objects (TNOs: Jewitt et al., 1992) has revolutionized the study of the solar system in the past decade. These objects orbit the Sun with orbital semi-major axes of 30 to 50 AU, typically have temperatures of  $\sim 75\,\text{K}$ , and are thought to be fossil remnants of the Sun's planetary accretion disk. Now over 400 are known with diameters ranging from 100 to 1000 km (see Schulz, 2002, for a review). Roughly there is one TNO per square degree brighter than  $m_R = 23.2$ , and the integral counts go as  $\log N(> m) = 0.63(m - m_o)$ , *i.e.* roughly  $N(> S) \propto S^{-1.6}$ , (Trujillo et al., 2001). TNO's were discovered with optical telescopes, but mm and submm observations are essential to understand them physically. For instance, the optical magnitudes constrain the product of

the TNO size and albedo; by measuring the thermal emission in the mm regime this degeneracy is broken. Jewitt et al. (2001) have used simultaneous SCUBA ( $850\,\mu\text{m}$ ) and optical observations to measure the albedo and radius of Kuiper Belt Object (20000) *Varuna*. They found an  $850\,\mu\text{m}$  flux density of  $\sim 2-3\,\text{mJy}$  (with an RMS of  $1\,\text{mJy}$  in 5 hours). This corresponds to  $150-250\,\mu\text{Jy}$  at  $3\text{mm}$ . A  $5\sigma$  detection on such an object will be obtained with the Penn Array in  $\sim 2$  minutes. The Penn Array should be capable of measuring the albedos and sizes of all known large TNOs fairly quickly. As Kuiper-Belt Objects go (20000) *Varuna* is fairly bright ( $m_R = 19.1$ ), and the question arises as to how deeply the GBT will be able to probe the population. A lower limit is set by extragalactic confusion: at  $30\,\mu\text{Jy}$  the Penn Array on the GBT has a maximum SNR per pixel of 5. One should then integrate to a thermal noise level of  $6\,\mu\text{Jy}$  RMS, which is reached in one hour. If the albedos are similar to (20000) *Varuna*, this corresponds to  $R$ -band apparent magnitudes in the range of 21 to 21.5. However these models are uncertain and if there were populations with lower albedos, mm observations would probe to fainter magnitudes.

It would also be possible, in principle, to use large arrays on the GBT to survey the sky for TNOs. It turns out that small, wide-field optical telescopes are much more efficient for this purpose. For instance the Kitt Peak  $0.9-m$  telescope with the  $1^\circ$  Mosaic camera reaches  $m_R = 21.8$  on  $1\,\text{deg}^2$  in one hour, deep enough to detect (20000) *Varuna* with an SNR of 50 and comparable to the confusion limit of the GBT at  $3\text{mm}$ . An  $80 \times 80$  array on the GBT would require 5 hours to map  $1\,\text{deg}^2$  to the sensitivity needed for a  $5\sigma$  detection of (20000) *Var*.

The GBT will also easily detect comets when they are still cold and icy and therefore provide information on how their surface characteristics change when they approach the Sun. For instance, Hale-Bopp was detected by BIMA at  $3\text{mm}$  with a peak flux density of  $13\,\text{mJy}$  per  $10''$  beam, with extended structure visible in the maps over tens of arcseconds (de Pater et al., 1998).

## 4 Galaxy Clusters & the Sunyaev-Zel'dovich Effect

Measurements of the Sunyaev-Zel'dovich Effect (SZE) have long been sought as a probe of cosmology (Birkinshaw, 1999). In the past decade these measurements have matured to the point where images of the SZE in large samples of galaxies have been obtained (Carlstrom et al., 1996; Reese et al., submitted), and Hubble constant estimates in samples at low- $z$  have become possible (Myers et al., 1997; Mason et al., 2001). High-angular resolution data from Chandra have greatly improved our understanding of these objects. They have revealed embedded cold blobs of gas which may be remnants of past merger activity (Markevitch et al., 2000), and enabled detailed study of ongoing subcluster mergers (eg Kempner et al., 2002). SZE observations are currently limited to a much lower resolution view of the Intra-Cluster Medium (ICM). When user instruments with suffi-

cent sensitivity become available, the SZE will provide a valuable independent, detailed view of these and other processes. As an example: it is clear that the dark-matter profile in galaxy clusters is not well-understood in detail since giant radial arcs are too abundant by a factor of 10 under currently accepted cosmologies (see, *e.g.*, Bartelmann et al., 1998). A high-resolution view of the baryons in clusters both relaxed and violent, orthogonal to the view provided by X-rays, will help clarify this situation. Beyond this, high-resolution, high-sensitivity maps of the SZE in more distant clusters, in combination with X-ray and weak-lensing data, will allow accurate estimates of the 3D structure and orientation of galaxy clusters (*e.g.* Zaroubi et al., 2001).

Another topic of emerging interest is the formation and evolution of structures at high- $z$ . Because the SZE surface brightness does not dim as a physical system moves further away (*i.e.*, it is not subject to “cosmological dimming”), the SZE is a uniquely suitable probe of this regime. Measurements of the abundance of galaxy clusters as a function of redshift also give strong constraints on the underlying cosmology. Recent CMB measurements on arcminute scales may already have detected this signal (Mason et al., 2003; Kuo et al., submitted; Dawson et al., submitted).

The degree of substructure in clusters as a function of mass and redshift is also a powerful constraint on cosmology and structure formation scenarios (*e.g.* Evrard et al., 2002; Bond et al., submitted); moreover, there are significant uncertainties in these scenarios which, if unresolved, may limit the scientific yield of future wide area SZ surveys. As an example, there is evidence from X-ray (*e.g.* Ponman et al., 1999) and SZ (McCarthy et al., in preparation) cluster scaling relations for an “entropy floor” in the ICM. The epoch and mechanism of this heating must be understood to accurately relate cosmological structure formations to the results of large-scale SZ surveys. Cluster morphology is a good diagnostic of the cluster entropy (Lloyd-Davies et al., 2000; Carlstrom et al., 2002). The Penn Array on the GBT will not have sufficient surface-brightness sensitivity (or available observing time) to conduct blind surveys for distant SZ clusters— with current and near-future instrumentation this requires dedicated observations. However it will easily *detect* distant clusters found with dedicated surveys (such as the SZA— Carlstrom et al. (2002)— or AMiBa— Lo et al. (2000)). The angular resolution provided by GBT/PAR observations will be valuable in tracing how these massive structures evolve.

The GBT’s angular resolution will be significantly greater than that of the instruments which currently dominate the field. For instance, BIMA at 1cm has a FWHM of  $\sim 40''$  in the compact configuration needed for interferometric SZE observations, as the aperture plane sampling on the long baselines is too dilute for good surface-brightness sensitivity. Nearby clusters are quite extended, with core radii of a few arcminutes to  $\sim 10'$ . Clusters at  $z = 1$  will have core radii of  $\sim 30''$  (less for poor systems), and since the angular diameter distance  $D_A(z)$  is approximately flat beyond this, higher redshift systems will have similar apparent sizes. For baryonic density profiles which asymptotically fall as  $1/r^2$  there is significant flux at radii well beyond  $r_{core}$ . The SZE from galaxy clusters is thus quite extended: if all of the flux within a virial radius can be recovered

a factor of 5 or more increase in signal-to-noise can be achieved. In mapping extended objects, the GBT's large aperture is of limited value. Poor systems at high- $z$ , however, may be expected to have core radii as small as  $\sim 15''$ , to which the GBT is well matched, and lower-resolution experiments will lose the peak of this signal by beam dilution. The GBT's large focal plane (see § 2.1) offers the possibility of extremely high mapping speeds for extended sources. Even with only 64 pixels competitive science can be done, as we illustrate. The key foreseeable competition will be from Bolocam-II, a 144 element 2.1-mm bolometer array on the LMT with  $\sim 19''$  (FWHM) angular resolution. The SZE is 25% stronger at 2.1-mm; overall, the LMT/Bolocam-II combination is then roughly three times as fast as the GBT/Penn Array for mapping extended SZ signals. An  $80 \times 80$  3mm array on the GBT would be 30 times as fast as Bolocam-II.

We now consider three specific cases: mapping a low- $z$ , Coma-like cluster; mapping the core of a relaxed, nearby cluster; and detecting high- $z$  clusters.

#### **SZE Observing Cases**

1. **Square-Degree SZE Maps** would be useful for projects such as mapping the SZE in the nearby Coma cluster of galaxies. Coma has a central inverse-Compton optical depth  $\tau = 5 \times 10^{-3}$  and  $kT_e = 9\text{keV}$ . This yields a Compton parameter  $y = 8.8 \times 10^{-5}$  which corresponds to a Rayleigh-Jeans decrement of  $475\mu\text{K}$ . We then have a 90 GHz surface brightness of  $163\mu\text{Jy}$  per  $8''$  (FWHM) beam, or an equivalent temperature (main-beam referenced antenna temperature) of  $\sim 312\mu\text{K}$  for the GBT. Note that although it is conventional to discuss the SZE in terms of a temperature decrement this can become confusing at high frequencies where the Rayleigh-Jeans approximation is poor so we will tend to stick to flux units. The Penn array will be able to map a  $1^\circ \times 1^\circ$  area to an  $80\mu\text{Jy}$  RMS in 14 hours, yielding a  $2\sigma$  measurement per pixel or a  $5\sigma$  measurement per  $20''$  resolution element. This is comparable to the time which modern high-bandwidth instruments require to measure the SZE in low- $z$  clusters (*e.g.*, the CBI spends about 15 hours per cluster, including a factor of 3 LEAD-MAIN-TRAIL overhead; OVRO/BIMA obtain maps in several 10's of hours, mostly due to the currently limited correlator bandwidth). An  $80 \times 80$  array would achieve this in 8 minutes. On large scales these maps will be dominated by intrinsic anisotropy.
2. **Arcminutes Square SZE Maps** would be useful for studying slightly more distant clusters at high resolution ( $z > 0.1$ ) or studying ICM structures in nearby clusters. Consider for example a  $5' \times 5'$  map. In 10 hours on this field the Penn Array will achieve an  $8\mu\text{Jy}$  RMS; an  $80 \times 80$  array would take only 6 minutes to do this. The core of a relaxed, rich galaxy clusters will typically have an electron number density  $n_e \sim 10^{-2}$  and  $T_e \sim 4\text{keV}$  for a Compton  $y = 1.6 \times 10^{-5}$  through the central 100 kpc. This gives  $\Delta S_\nu = 29\mu\text{Jy}$  per  $8''$  beam ( $\Delta T_{RJ} = 86\mu\text{K}$ ). Our  $5' \times 5'$  map will have an SNR of 5 with  $15''$  resolution. The total decrement in the center of such a cluster will approach  $185\mu\text{Jy}$  per beam. An infalling group of galaxies such as that in A85 can be expected to have a signal

$\sim 2$  times fainter, so with half the resolution or four times the integration time similar results can be obtained. Rich clusters at moderate redshifts have signals similar in strength to nearby clusters and the 10 hour map described above would provide the highest resolution cluster images to date.

3. **Distant Cluster Searches** Consider a search for structures with virial masses  $M_{200} = 1.25 \times 10^{14} h^{-1} M_{sun}$ , one-sixth the mass of Coma. The abundances of such clusters are expected to be between 0.4 and 1.6  $\text{deg}^{-2}$  for  $\Lambda\text{CDM}$  cosmologies and assuming  $\sigma_8$  values between 0.85 and 1.04 (Evrard et al., 2002); less massive systems are much more abundant, and more massive systems much less abundant. Using Coma-normalized mass-temperature relation  $T_e = 9(M/M_{coma})^{2/3} \text{ keV}$ , we expect an electron (virial) temperature of  $\sim 3 \text{ keV}$ . Typical inverse-compton optical depths for nearby clusters without cooling flows are  $\tau \sim 4 \times 10^{-3}$ , and this is seen to be approximately independent of mass (this can be justified on virialization grounds: clusters bloat when they accrete more mass, which reduces the surface brightness). This yields central compton- $y$  parameters of  $y \sim 2.3 \times 10^{-5}$  or  $\Delta S_\nu = 42 \mu\text{Jy}$  per GBT beam. In a  $\sigma_8 = 1.04$  universe you must survey  $3 \text{ deg}^2$  to detect even 5 such clusters. To a depth of  $1\sigma$  per pixel ( $5\sigma$  overall) this takes 150 hours (an  $80 \times 80$  array would do it in 1.5 hours). Given the demand for GBT 3mm time, and real-world uncertainties such as the value of  $\sigma_8$ , this is probably not a winning application. Nevertheless were this cluster detected by one of the dedicated surveys, high-resolution images of a  $5' \times 5'$  region surrounding it could be obtained by the GBT in 6 hours. This map would have a SNR of 4 per  $8''$  pixel. Note the virial radius is  $r_{200} \sim 1 h^{-1} \text{ Mpc}$  which for  $\Lambda\text{CDM}$  translates into  $3'$  at  $z = 1$ . The assumptions which went into this estimate are somewhat uncertain (*e.g.*, would typical low-mass systems at the relevant redshift be virialized? how does the central inverse-Compton optical depth scale with mass at high  $z$ ?) but this is one of the arguments for high resolution SZ imaging.

## 5 The Origin & Evolution of Galaxies

A significant fraction of the total electromagnetic energy density in the Universe originating from visible galaxies resides in the present-day millimeter and sub-mm wavebands, owing to dust absorption and the effects of a cosmological redshift. Results in the  $850 \mu\text{m}$  and  $450 \mu\text{m}$  bands from SCUBA on the JCMT in the past decade have revolutionized our understanding of galaxies at high redshift by giving an orthogonal picture to that provided by optical techniques, principally Lyman-break selection (Steidel et al., 1996; Giavalisco, 2002). Sub-mm and mm observations have the advantage, compared to the optical, of not being affected by dust obscuration. Beyond this, at wavelengths from  $\sim 3 \text{ mm}$  to  $\sim 850 \mu\text{m}$  the rising SEDs expected of dusty ULIRGs almost exactly cancel



the diminution of flux density with increasing redshift due to the increasing luminosity distance  $D_L(z)$ . For these reasons SCUBA observations, as well as longer wavelength observations with the IRAM 30-m, have been instrumental in revealing a population of extremely IR-luminous galaxies over the range  $1 < z < 4$ ; this is in contrast to optical observations, which at first had seemed to suggest a peak in the star formation rate at  $z \sim 1.5$ .

A significant limitation of the SCUBA observations, is their angular resolution. The GBT at 3mm will have higher resolution ( $8''$ ) than the two telescopes which currently dominate the field, SCUBA ( $15''$  at the workhorse frequency) and the IRAM 30m ( $11''$ ). This will enable observers to probe systems  $\sim \sqrt{2}$  times less massive due to reduced confusion; where already optically thick at submm wavelengths, the 3mm mass limit will be deeper still. The GBT's increased resolution will probably not be of great help in securing optical IDs since even sub-arcsecond resolution is often not sufficient to yield unambiguous results (Hughes et al., 2002). Interferometric follow-up, *e.g.* with CARMA, ALMA, or the SMA, will continue to be needed.

Many sub-mm selected systems do not even have optical counterparts due to dust obscuration. There has consequently been great interest in photometric methods of determining the redshifts (*e.g.* Carilli & Yun, 1999; Hughes et al., 2002). One difficulty with these techniques is degeneracies between model parameters (Blain et al., 2003); for this reason, it is important to probe the SEDs of target objects over a wide range of frequencies. A 3mm data point in combination with 2mm or 1mm data would fairly cleanly measure the dust opacity index  $\beta$  and improve constraints on the redshift  $z$ .

The GBT's real strength is in large area surveys for point sources and here, in spite of the comparatively low frequency, the GBT has an advantage over IRAM and SCUBA surveys due to sheer sensitivity. As an example we consider the Hughes et al. (1998)  $850\mu\text{m}$  map of the Hubble Deep Field. They observed a  $9\text{ arcmin}^2$  region to an RMS of  $0.45\text{ mJy}$ ; this took 50 hours of telescope time in excellent atmospheric conditions. At the detection threshold of  $2\text{ mJy}$  these observations are confusion limited. Assuming a dust opacity  $\beta = 1.35$  and  $T_d = 58\text{ K}$  (Yun & Carilli, 2002) and averaging over  $1 < z < 4$ , the ratio  $S_{850\mu\text{m}}/S_{3\text{mm}} \sim 50$ . To probe a similar physical population, the 3mm observations would then need to go down to  $40\mu\text{Jy}$ . The PAR/GBT can map  $3' \times 3'$  to  $10\mu\text{Jy}$  RMS in two hours, *i.e.*, 25 times faster than SCUBA. An  $80 \times 80$  array on the GBT would do this in less than two minutes.

The GBT will also be capable of large-area surveys for ultra-luminous dusty galaxies at high redshift. Constraints at high flux densities (*e.g.* Scott et al., 2002; Carilli et al., 2001) are currently limited by the mapping speed of single-dishes, and arrays on the GBT will significantly improve this. There are also constraints at brighter flux densities from ISO at  $90\mu\text{m}$  (Efstathiou et al., 2000), but these results are not sensitive to sources at  $z > 1$  or so. Consider the ELAIS (ISO) survey of  $12\text{ deg}^2$  conducted by Efstathiou et al. (2000). An  $80 \times 80$  array on the GBT could map such a region to  $200\mu\text{Jy}$  RMS in about 6 hours (Penn Array: 56 hours), yielding about 180 sources brighter than  $1\text{ mJy}$  or so. This is similar to the number of sources detected by Efstathiou et al. (2000) in their

IR survey, but high- $z$  galaxies will be more strongly represented.  $S_{3mm} = 1$  mJy is roughly equivalent to  $S_{850\mu m} \sim 50$  mJy; current SCUBA surveys only cover enough area to go up to  $S_{850} \sim 10$  mJy, and then only with large error bars. A massive SCUBA survey is currently underway which will improve these constraints (SHADES). The SHADES survey will use 180 shifts of UK SCUBA time over the next 3 years, producing (in 1000 hours of telescope time or roughly 500 hours of integration) an  $850\mu m$  map of a half square degree with an RMS of 2 mJy. This field will also be targeted by BLAST. The Penn Array on the GBT will do this in 25 hours of integration ( $80 \times 80$  array: 15 minutes). Again, the GBT observations will be sensitive to galaxies at redshifts higher than either BLAST or SCUBA can detect.

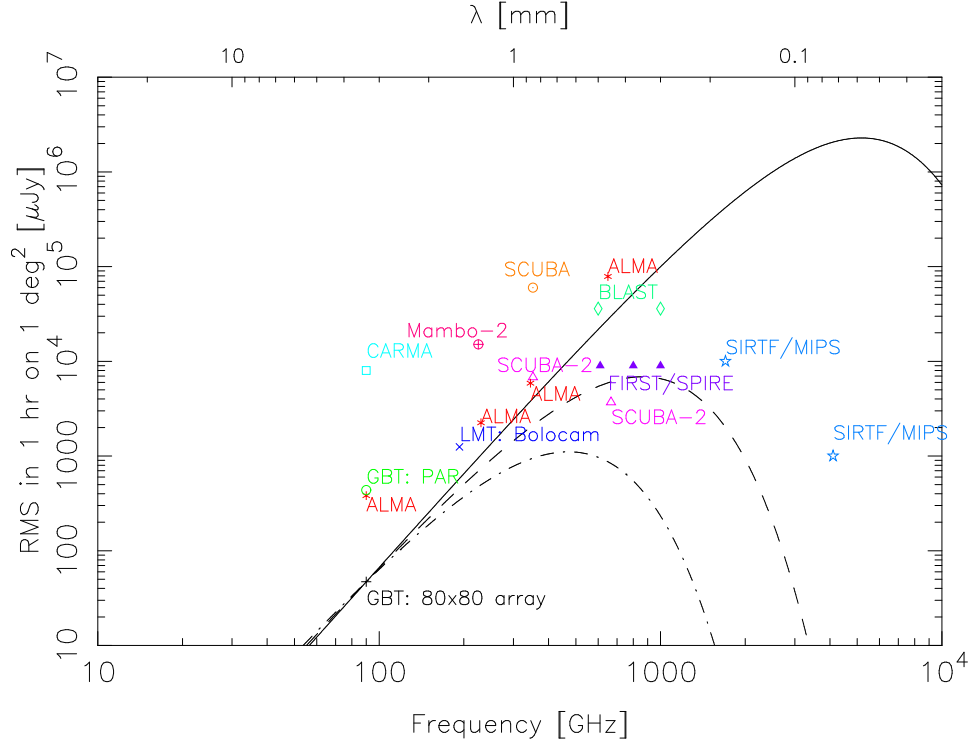


Figure 3: Expected performance of an  $80 \times 80$  3mm array on the GBT for discovering high-redshift galaxies. As before the curves are for  $z = 0$ ,  $z = 5$ , and  $z = 10$ . For  $z > 7$  a large 3mm array on the GBT will be faster than any existing or planned instrument.

The combination of a small beam and high point-source mapping speed will enable the GBT to measure high- $z$  galaxy counts over the widest range of flux densities currently possible. These measurements would yield important constraints on the SEDs of high- $z$  galaxies. SED templates are currently based on samples of low-redshift galaxies and are important for photometric redshift esti-

mates. The mm observations will also constrain the abundance of dusty galaxies at high redshifts, a currently unexplored topic. When operational, BOLOCAM-II on the LMT will be  $\sim 5$  times as fast as the GBT/PAR combination for a  $z = 5$  source; an  $80 \times 80$  array on the GBT would be two to four times as fast as LMT/BOLOCAM-II. For sources at  $z > 7$  a large array on the GBT is faster than any planned instrument (see Figure 3).

## 6 Summary & Conclusions

A major new capability such as mm wave operation on a 100-m aperture telescope will have a wide range of impacts in many fields. As an instrument with a wide base of users with a diversity of interests this is important; however it is difficult to consider every possible project, and so I have only examined a few clear areas of great current interest. Perhaps most interesting are the unexpected areas of research which will be made possible, but these are hard to assess.

Generally it is clear that as a hundred-meter telescope the GBT's near-term unique advantage is collecting area, and hence point source sensitivity. With bolometer cameras this is leveraged, potentially very greatly, into a high point source survey speed. In the 3mm continuum it is most natural to observe targets which are approximately thermal, and it is best to observe those which are cold or highly redshifted. The GBT has higher resolution than other mm and sub-mm single-dishes—an advantage for point-source work, which is often confusion-limited, and for follow-up on sources (*e.g.*, detected by comparatively low-resolution satellites like SIRTf) which are either too faint or too extended to follow up with mm and sub-mm interferometers. As a single dish, the GBT can be expected to provide an important complementary view (*e.g.*, of Galactic molecular clouds, or nearby galaxies) to the highly filtered view that interferometers provide. It is as important to note that the GBT does not have a significant competitive advantage in mapping large areas to find extended objects. Here dish size does not matter once you fill the beam, and there are a number of mm telescopes with as many or more pixels than the Penn Array (or for that matter, the notional  $80 \times 80$  array) likely to be fielded on comparable timescales. Once found, it will be desirable to follow up these extended objects at higher resolution, and here bolometer arrays on a big single dish are useful. Large-format arrays typically use Lyot stops to define the aperture illumination and so will not have beams as clean as those by feedhorn arrays, but due to the lack of obstruction the GBT beam can be expected to be cleaner than that of similar receivers on other telescopes such as the JCMT or LMT.

We have discussed many areas where bolometer arrays on the GBT can be expected to contribute. Some highlights are:

- Photometry of solar system objects (§ 3.4). The GBT will quickly measure thermal emission from main-belt asteroids and TNOs, enabling one to measure the sizes and albedos of large samples of objects. This is fun-

damentally a point source observation so the Penn Array delivers most of the science and no large array is needed.

- Accretion/debris disks around young stars (§§ 3.2, 3.3). The Penn Array on the GBT will have sufficient sensitivity to quickly map young stars and Vega-like stars. Together with shorter wavelength observations, *e.g.* from SIRTf, this will be an excellent probe of grain properties and grain evolution. The GBT also, again, has higher resolution than any current instrument except for the interferometers, which will be limited by sensitivity. These disks are typically small ( $\sim 1'$  or less) and this is not a key driver for a large format array.
- Searches for cold protostellar clouds in the Galaxy (§ 3.1). The Penn Array on the GBT will be sensitive enough for blind surveys of many square degrees of the Galactic plane. This would yield an unbiased census of cold pre-protostellar clouds, and be complementary to future submm and CO surveys of the Galaxy. The Penn Array is likely to be the first ground-based instrument with sufficient sensitivity to do such surveys; the SIRTf GLIMPSE Legacy project will also do such a survey, although in the far infrared. Infrared surveys would be less sensitive to cold clouds. Eventually SCUBA-2 and the LMT will be faster than the GBT for long-wavelength searches due to larger beams and more advantageous observing frequencies, and so these searches are probably not a key motivation for large format arrays. The Penn Array will be an ideal instrument to follow up on SIRTf/MIPS, SCUBA-2, and LMT discoveries at higher resolution and lower frequency. A large-format array would be even better for follow-up since these objects are quite extended.
- Mapping Low-Mass Star Forming Cores (§ 3.1) The GBT will, much more quickly than is currently possible, make complete, high-resolution images of star forming to a greater distance than is currently feasible.
- SZE in Distant Clusters (§ 4). Planned dedicated surveys (SZA, AMiBa, AMI, ACT, SPT, APEX) will in the next few years discover and catalog many dozens of high redshift clusters. However these experiments typically have a resolution of  $1'$  (FWHM) or worse, which at  $z = 1$  corresponds to a resolution of  $350 h^{-1}$  kpc and will thus lack the resolution for detailed studies of the cluster morphologies (*e.g.* merger fraction as a function of redshift). In addition a significant uncertainty in the cosmological interpretation of the surveys is introduced by our ignorance of the epoch and mechanisms for entropy injection and feedback from small scales. Cluster morphology is one diagnostic of this, and SZ will be the best way to get the morphology for clusters beyond  $z \sim 1$ . For these studies a resolution of  $100 h^{-1}$  kpc or so is desired, especially for the poor systems where feedback is likely to be more important. An SZ map of even a fairly poor system takes 10 to 20 hours with the Penn Array on the GBT, in line with what is achieved with other modern instruments; an  $80 \times 80$  array would

do this in a matter of minutes. Since the SZ signals even from distant clusters are rather extended GBT SZ observations would benefit from a larger format array. This is a potentially significant motivation for a large bolometer array.

- Photometric Redshift Support (§ 5). The Penn Array on the GBT will have enough sensitivity to effectively complement continuum surveys by BLAST, SCUBA/SHADES, and eventually the LMT. By providing 3mm coverage the photometric redshift estimates will be improved. These measurements could revolutionize our understanding of galaxy formation. With a large format array these observations would remain useful for the foreseeable future.
- Continuum surveys for high redshift galaxies (§ 5). These will go deeper than current surveys, which are confusion-limited, and will provide the first constraints on counts at 3mm, which will tell us about the SEDs. The Penn Array on the GBT will, for  $z > 5$  targets, be roughly as sensitive as BLAST and SIRTf, and more sensitive than SCUBA or MAMBO-2—in all cases however, the GBT will probe more deeply due to its smaller beam. The PAR/GBT will also be more sensitive to high-redshift galaxies; Bolocam-2 on the LMT will at some point become more preeminent, but the long-wavelength information from the GBT will still be desirable. These surveys will enable new constraints on high- $z$  galaxy SEDs, on the number counts over an unprecedentedly large range of luminosities, and on the correlation function of the sources (a major target of SHADES, to test the ULIRG/elliptical hypothesis). An  $80 \times 80$  array on the GBT is more sensitive to  $z > 7$  dusty galaxies than any existing or planned instrument including SCUBA-2. The nominal expectation is that such systems are rare since metals are needed to form dust, and the metallicities at such high redshifts must be lower than at present. However the data not unambiguously support this expectation: Armus et al. (1998) have detected dust in the  $z = 5.34$  galaxy RD1 and there are others, including the most recent detection at  $z = 6.4$  (Walter *et al.*, submitted); Thuan et al. (1999) have measured high levels of IR dust emission in the extremely metal-poor dwarf galaxy SBS 0335-052; and WMAP (Kogut et al., submitted) has revealed a probable epoch of star-formation activity at  $z \sim 15$  or higher so the ISM is probably be polluted with metals at an early time. This is a potentially major motivation for a large array which plays to the unique strengths of the GBT.

The last is clearly a key area. To illustrate this, consider that current results in this field are dominated by SCUBA (mostly  $850 \mu\text{m}$ ) and MAMBO surveys; together these telescopes have detected mm/sub-mm emission from only about 200 sources, and of these, only  $\sim 20\%$  are detected at greater than  $5\sigma$  (D. Hughes, private communication). For further progress (statistical samples; measuring the correlation function of sources; *etc.*) many more sources are needed. The Penn Array should be able to measure  $8' \times 8'$  to  $50 \mu\text{Jy}$  ( $5\sigma$ ) in 15 hours and

doubling the number of sources known at  $5\sigma$ ; a  $20' \times 20'$  of comparable depth should be obtained in 80 hours, doubling the number of sources known to 400, in this case, however, all to  $5\sigma$ . A large format array on the GBT, in contrast, is expected to discover *as many “sub-mm” galaxies as are currently known every  $\sim 2$  hours*. This would be an efficient use of the GBT’s mm capabilities at a site where observing time is limited. Wider, shallower surveys for rare objects could also be conducted; these would have a lower source discovery rate, but are of great scientific interest.

Beyond the specific applications we have examined, a strong multi-frequency continuum capability is essential for many fields and will have a wide range of impacts. Large arrays on the GBT would be groundbreaking on this front. Continuum surveys such as the NVSS (Condon et al., 1998) have had substantial and long-lasting impacts reaching well beyond their initial science drivers.

There is potentially a very great payoff from large bolometer arrays on the GBT. However there are many challenges which must be overcome. These include achieving 3mm operation with the telescope; realizing good performance with TES arrays in the field; demonstrating useful operational efficiency at the Green Bank site; and optimizing the analysis algorithms to come close to the thermal noise limit in the continuum maps. When these issues have been dealt with many of the open scientific questions in the above discussion should be answered and it will be clear whether or not pursuing a more ambitious bolometer instrument makes sense. The science for such an instrument would also be nicely complemented by a wideband correlator (“redshift machine”).

**Acknowledgements:** Much of the material in § 3 is based on an early draft science case for GBT Bolometer Arrays written by Goran Sandell. The author thanks Bill Cotton, Don Wells, and Fred Schwab for many discussions about array imaging and observing strategies.

## A Appendix: Other Instruments

A collection of other instruments is presented below. Where appropriate, the raw numbers used as the basis for sensitivity estimates are also given.

- **LMT/Bolocam** is expected to have a per-detector NEFD of  $2 \text{ mJy} \sqrt{\text{sec}}$  at 220 GHz; there are 151 detectors, and the beamsize is  $8''$ . LMT construction is scheduled to be finished by the end of 2004, with science operations starting about a year later [LMT Bolocam Summary web page]
- **JCMT/SCUBA** has a per-detector (point source) sensitivity of  $90 \text{ mJy} \sqrt{\text{sec}}$ . There are 37 detectors at  $850 \mu\text{m}$  and the beam is  $15''$  (FWHM). [SCUBA web page]
- **JCMT/SCUBA-2** will be able to map  $2.8 \text{ deg}^2$  to a  $10 \text{ mJy}$  RMS at  $850 \mu\text{m}$  in one hour; it will be able to map  $7.2 \text{ deg}^2$  to  $10 \text{ mJy}$  in the same time. SCUBA-2 is currently scheduled to be fully installed on the JCMT in late 2006 [SCUBA-2 web page]

- **ALMA** achieves a peak point source sensitivity in 60 seconds of (27, 71, 120, 849)  $\mu\text{Jy}$  at (90, 230, 345, 650) GHz; these are the first light bands. The antenna diameter is 12m so the primary beam diameters are about (66, 29, 19, 10)" (*FWHM*). ALMA interim operations are scheduled to begin in 2006, with full science operations by the end of 2010 [ALMA publicity pamphlet & project book]
- **MAMBO-2 on IRAM** has a per-detector noise level of 50 mJy  $\sqrt{\text{sec}}$  at 1.2mm and 117 detectors. The beamsize is 11". [IRAM web page]
- **CARMA** in 5 hours of integration on a single pointing will achieve a peak point source sensitivity of (40, 100, 700)  $\mu\text{Jy}$  at (100, 230, 345) GHz. Most of this sensitivity comes from the 10.4m (OVRO) antennas, and for these, the primary beam width at 3mm is 77". CARMA is scheduled to be fully operational in 2005 [Robinson talk by J. Carpenter, Dec 2001, via Al Wootten's web page; schedule from CARMA web page]
- **BLAST** will achieve a  $1\sigma$  sensitivity of 36 mJy in 1 hour map of a  $1 \text{ deg}^2$  region at each of 350 and 500  $\mu\text{m}$ . The beam widths are 59" and 41", respectively. BLAST has its first flight in 2003 [Devlin et al., astro-ph/00123271]
- **SIRTF/MIPS** will achieve a  $5\sigma$  rms of 1.4 mJy in 500 sec at 70  $\mu\text{m}$  on a single ( $5'.2 \times 5'.2$ ) FOV. At 160  $\mu\text{m}$  MIPS will be confusion limited in a few seconds per FOV ( $5'.3 \times 0'.5$ ) and sensitivity is basically irrelevant. The beamsizes are 20" and 45"; the  $1\sigma$  confusion levels are 0.5 – 1.3 mJy and 7 – 19 mJy for 70 and 160  $\mu\text{m}$ , respectively. At 70  $\mu\text{m}$  Galactic Cirrus and Zodiacal light dominate, whereas at 160  $\mu\text{m}$  distant dusty galaxies dominate. SIRTF is scheduled for launch in mid-August 2003 [SIRTF Science Center Web Page and SIRTF Observer's Manual Chapter 8]
- **HERSCHEL/SPIRE** will achieve a  $5\sigma$  point source detection limit of 3 mJy at each of (250, 350, 500)  $\mu\text{m}$  in one hour. At each band the same  $4' \times 4'$  FOV is imaged. The beamsize will range from  $\sim 19''$  (250  $\mu\text{m}$ ) to  $\sim 38''$  (500  $\mu\text{m}$ ). Herschel is scheduled to launch in 2007 together on the same vehicle as Planck [ESA Herschel Web page]
- **SPT/Princeton Atacama Cosmology Telescope** These are both 10-m class telescopes with  $\sim 1000$  pixels in the 1 to 2 mm range. Both will come online sometime after 2006, and will be dedicated primarily to SZ surveys.
- **APEX** Is a mm/submm telescope using a 12m on-axis cassegrain (an ALMA prototype) antenna on the Chajnantour site. It will have  $\sim 300$  pixel TES bolometer arrays at 2mm and 870  $\mu\text{m}$ . At 2mm the beam is 40" (fwhm), and it is expected to come online in 2004. This would make it the first TES array used for collecting real astronomy.

Mapping speeds do not take into account observing overheads; the on-the-fly techniques likely to be employed by arrays on large telescopes should come reasonably close to achieving this.

## References

- Altenhoff, W. J., Baars, J. W. M., Wink, J. E., & Downes, D. 1987, *A&A*, 184, 381
- Armus, L., Matthews, K., Neugebauer, G., & Soifer, B. T. 1998, *ApJL*, 506, L89
- Aspin, C., Sandell, G., & Weintraub, D. A. 1994, *A&A*, 282, L25
- Bartelmann, M., Huss, A., Colberg, J. M., Jenkins, A., & Pearce, F. R. 1998, *A&A*, 330, 1
- Beckwith, S. V. W., Sargent, A. I., Chini, R. S., & Guesten, R. 1990, *AJ*, 99, 924
- Birkinshaw, M. 1999, *Phys.Rept.*, 310, 97
- Blain, A. W., Barnard, V. E., & Chapman, S. C. 2003, *MNRAS*, 338, 733
- Blain, A. W., Smail, I., Ivison, R. J., Kneib, J.-P., & Frayer, D. T. 2002, *Phys.Rep.*, 369, 111
- Bond, J., Contaldi, C. R., Pen, U.-L., Pogosyan, D., Prunet, S., Ruetalo, M. I., Wadsley, J. W., Zhang, P., Mason, B. S., Myers, S. T., Pearson, T. J., Readhead, A. C. S., Sievers, J. L., & Udomprasert, P. S. submitted, *ApJ*, astro-ph/0205386
- Carilli, C. L., Owen, F., Yun, M., Bertoldi, F., Bertarini, A., Menten, K. M., Kreysa, E., & Zylka, R. 2001, in *Deep Millimeter Surveys: Implications for Galaxy Formation and Evolution*, 27–+
- Carilli, C. L. & Yun, M. S. 1999, *ApJL*, 513, L13
- Carlstrom, J. E., Holder, G. P., & Reese, E. D. 2002, *ARA&A*, 40, 643
- Carlstrom, J. E., Joy, M., & Grego, L. 1996, 456, L75
- Condon, J. J., Cotton, W. D., Greisen, E. W., Yin, Q. F., Perley, R. A., Taylor, G. B., & Broderick, J. J. 1998, *AJ*, 115, 1693
- Dawson, K., Holzapfel, W., Carlstrom, J., LaRoque, S., Miller, A., Nagai, D., & Joy, M. submitted, *ApJ*, astro-ph/0206012
- de Pater, I., Forster, J. R., Wright, M., Butler, B. J., Palmer, P., Veal, J. M., A’Hearn, M. F., & Snyder, L. E. 1998, *AJ*, 116, 987
- Efstathiou, A., Oliver, S., Rowan-Robinson, M., Surace, C., Sumner, T., Héraudeau, P., Linden-Vørnle, M. J. D., Rigopoulou, D., Serjeant, S., Mann, R. G., Cesarsky, C. J., Danese, L., Franceschini, A., Genzel, R., Lawrence, A., Lemke, D., McMahon, R. G., Miley, G., Puget, J.-L., & Rocca-Volmerange, B. 2000, *MNRAS*, 319, 1169



- Evrard, A. E., MacFarland, T. J., Couchman, H. M. P., Colberg, J. M., Yoshida, N., White, S. D. M., Jenkins, A., Frenk, C. S., Pearce, F. R., Peacock, J. A., & Thomas, P. A. 2002, *ApJ*, 573, 7
- Fixsen, D. J., Moseley, S. H., & Arendt, R. G. 2000, *ApJS*, 128, 651
- Giavalisco, M. 2002, *ARA&A*, 40, 579
- Greaves, J. S., Holland, W. S., Moriarty-Schieven, G., Jenness, T., Dent, W. R. F., Zuckerman, B., McCarthy, C., Webb, R. A., Butner, H. M., Gear, W. K., & Walker, H. J. 1998, *ApJL*, 506, L133
- Henning, T., Burkert, A., Launhardt, R., Leinert, C., & Stecklum, B. 1998, *A&A*, 336, 565
- Hogerheijde, M. R., Jayawardhana, R., Johnstone, D., Blake, G. A., & Kessler, J. E. 2002, *AJ*, 124, 3387
- Holdaway, M., Owen, F., & Rupen, M. 1994, *Alma Memo* 123
- Holland, W. S., Greaves, J. S., Dent, W. R. F., Wyatt, M. C., Zuckerman, B., Webb, R. A., McCarthy, C., Coulson, I. M., Robson, E. I., & Gear, W. K. 2003, *ApJ*, 582, 1141
- Holland, W. S., Greaves, J. S., Zuckerman, B., Webb, R. A., McCarthy, C., Coulson, I. M., Walther, D. M., Dent, W. R. F., Gear, W. K., & Robson, I. 1998, *Nature*, 392, 788
- Hughes, D. H., Aretxaga, I., Chapin, E. L., Gaztañaga, E., Dunlop, J. S., Devlin, M. J., Halpern, M., Gundersen, J., Klein, J., Netterfield, C. B., Olmi, L., Scott, D., & Tucker, G. 2002, *MNRAS*, 335, 871
- Hughes, D. H., Serjeant, S., Dunlop, J., Rowan-Robinson, M., Blain, A., Mann, R. G., Ivison, R., Peacock, J., Efstathiou, A., Gear, W., Oliver, S., Lawrence, A., Longair, M., Goldschmidt, P., & Jenness, T. 1998, *Nature*, 394, 241
- Jewitt, D., Aussel, H., & Evans, A. 2001, *Nature*, 411, 446
- Jewitt, D., Luu, J., & Marsden, B. G. 1992, *IAUC*, 5611, 1
- Johnstone, D. & Bally, J. 1999, *ApJL*, 510, L49
- Kempner, J. C., Sarazin, C. L., & Ricker, P. M. 2002, *ApJ*, 579, 236
- Koerner, D. W., Sargent, A. I., & Beckwith, S. V. W. 1993, *ApJL*, 408, L93
- Kogut, A. et al. submitted, *ApJ* (astro-ph/0302213)
- Kuo, C., Ade, P., Bock, J., Cantalupo, C., Daub, M., Goldstein, J., Holzapfel, W., Lange, A., Lueker, M., Newcomb, M., Peterson, J., Ruhl, J., Runyan, M., & Torbet, E. submitted, *ApJ*, astro-ph/0212289

- Lloyd-Davies, E. J., Ponman, T. J., & Cannon, D. B. 2000, MNRAS, 315, 689
- Lo, K. Y., Chiueh, T., Liang, H., Ma, C. P., Martin, R., Ng, K.-W., Pen, U. L., & Subramanyan, R. 2000, in IAU Symposium
- Mannings, V. 1994, MNRAS, 271, 587
- Mannings, V., Koerner, D. W., & Sargent, A. I. 1997, Nature, 388, 555
- Markevitch, M., Ponman, T. J., Nulsen, P. E. J., Bautz, M. W., Burke, D. J., David, L. P., Davis, D., Donnelly, R. H., Forman, W. R., Jones, C., Kaastra, J., Kellogg, E., Kim, D.-W., Kolodziejczak, J., Mazzotta, P., Pagliaro, A., Patel, S., Van Speybroeck, L., Vikhlinin, A., Vrtilek, J., Wise, M., & Zhao, P. 2000, ApJ, 541, 542
- Mason, B. S., Myers, S. T., & Readhead, A. C. S. 2001, ApJL, 555, L11
- Mason, B. S., Pearson, T. J., Readhead, A. C. S., Shepherd, M. C., Sievers, J. L., Udomprasert, P. S., Cartwright, J. K., Farmer, A. J., Padin, S., Myers, S. T., Bond, J. R., Contaldi, C. R., Pen, U.-L., Prunet, S., Pogosyan, D., Carlstrom, J. E., Kovac, J., Leitch, E. M., Pryke, C., Halverson, N. W., Holzappel, W. L., Altamirano, P., Bronfman, L., Casassus, S., May, J., & Joy, M. 2003, ApJ, astro-ph/0205384
- McCarthy, I., Holder, G., Babul, A., & Balogh, M. in preparation, astro-ph/0303451
- Motte, F., Andre, P., & Neri, R. 1998, A&A, 336, 150
- Myers, S. T., Baker, J. E., Readhead, A. C. S., Leitch, E. M., & Herbig, T. 1997, 485, 1
- Norrod, R. & Srikanth, S. 1999, GBT Memo 199
- Olmi, L. 2001, A&A, 374, 348
- Paresce, F. & Burrows, C. 1987, ApJL, 319, L23
- Ponman, T. J., Cannon, D. B., & Navarro, J. F. 1999, Nature, 397, 135
- Reese, E., Carlstrom, J. E., Joy, M., Mohr, J., Grego, L., & Holzappel, S. submitted, ApJ., astro-ph/0205350
- Rohlfs, K., Wilson, T. L., & Huettmeister, S. 2000, Tools of radio astronomy (Tools of radio astronomy / K. Rohlfs, T.L. Wilson. New York : Springer, 2000. (Astronomy and astrophysics library,ISSN0941-7834))
- Sandell, G. & Weintraub, D. A. 1994, A&A, 292, L1
- Schulz, R. 2002, A&AR, 11, 1

- Scott, S. E., Fox, M. J., Dunlop, J. S., Serjeant, S., Peacock, J. A., Ivison, R. J., Oliver, S., Mann, R. G., Lawrence, A., Efstathiou, A., Rowan-Robinson, M., Hughes, D. H., Archibald, E. N., Blain, A., & Longair, M. 2002, MNRAS, 331, 817
- Shirley, Y. L., Evans, N. J., & Rawlings, J. M. C. 2002, ApJ, 575, 337
- Simon, M. & Guilloteau, S. 1992, ApJL, 397, L47
- Smail, I., Ivison, R. J., & Blain, A. W. 1997, ApJL, 490, L5+
- Srikanth, S. 1991, GBT Memo 67
- Steidel, C. C., Giavalisco, M., Pettini, M., Dickinson, M., & Adelberger, K. L. 1996, ApJL, 462, L17+
- Stompor, R., Balbi, A., Borrill, J. D., Ferreira, P. G., Hanany, S., Jaffe, A. H., Lee, A. T., Oh, S., Rabii, B., Richards, P. L., Smoot, G. F., Winant, C. D., & Wu, J. P. 2002, Phys.Rev.D, 65, 22003
- Testi, L. & Sargent, A. I. 1998, ApJL, 508, L91
- Thuan, T. X., Sauvage, M., & Madden, S. 1999, ApJ, 516, 783
- Trujillo, C. A., Jewitt, D. C., & Luu, J. X. 2001, AJ, 122, 457
- Weintraub, D. A., Sandell, G., & Duncan, W. D. 1989a, ApJL, 340, L69
- Weintraub, D. A., Sandell, G., Huard, T. L., Kastner, J. H., van den Ancker, M. E., & Waters, R. 1999, ApJ, 517, 819
- Weintraub, D. A., Zuckerman, B., & Masson, C. R. 1989b, ApJ, 344, 915
- Yun, M. S. & Carilli, C. L. 2002, ApJ, 568, 88
- Zaroubi, S., Squires, G., de Gasperis, G., Evrard, A. E., Hoffman, Y., & Silk, J. 2001, ApJ, 561, 600